Conformational Properties of α-Tubulin Tail Peptide: Implications for Tail−Body Interaction

Debnath Pal,[§] Pradip Mahapatra,[§] Tapas Manna,[§] Pinak Chakrabarti,[§] Bhabatarak Bhattacharyya,[§] Anirban Banerjee,[§] Gautam Basu,[‡] and Siddhartha Roy*,[‡]

Department of Biochemistry and Department of Biophysics, Bose Institute, P-1/12 CIT Scheme VIIM, Calcutta 700 054, India

ABSTRACT: The carboxy-terminal segments of the α/β-tubulins are flexible regions rich in acidic amino acid residues. It is generally believed that these regions play crucial roles in tubulin polymerization and interaction with many ligands, including colchicine. Exactly how these effects are exerted are not known at present. One such interesting aspect is the pH dependence of colchicine−tubulin interaction and the influence of the α-tail on the binding interaction. We have investigated the location of the colchicine-binding site on tubulin by docking. It has been located on the α/β interface on the N-terminal side, which is also supported by much of the solution data. This location is too far from the tail regions, suggesting that influence of the tail region is transmitted by a pH-dependent conformational change. Two-dimensional NMR studies indicate that at pH 7 a 13-residue peptide corresponding to α-tubulin tail shows little NOE constraints, suggesting extended conformation. On the contrary, at pH 5, a relatively compact structure was deduced from the interproton NOE constraints. Pulsed field gradient measurement of diffusion constant indicates that the peptide at pH 5 is substantially faster diffusing than at pH 7. The Perrin factors calculated from diffusion data indicates that the peptide structure at pH is significantly more compact than at pH 7. Temperature coefficients of several amide protons at pH 5 fall below 5 ppb/°K, indicating a degree of protection. A difference is also seen in the CD spectra obtained at different pHs, consistent with the NMR data. We have investigated the probable spatial organization of the tail of the α-subunit of tubulin, in the high pH extended form and the low pH compact form. On the basis of correlation of pH dependence of many properties of tubulin and the conformation of the α-tail peptide, we propose that the intrinsic conformational preference of the tail-region modulate the tail−body interaction, which in turn has important bearing on colchicine binding properties.

Tubulin, the major constituent of microtubules, polymerizes with help of accessory proteins (MAPs), to form the cytoskeletal elements that are essential for cell division and intracellular transport in all eukaryotes. In vitro, in absence of the accessory proteins, tubulin can be polymerized in the presence of monocations such as Mg^{2+}, Na^+ (*1, 2*), polycations (*3, 4*), and other agents such as glutamate, Taxol, and DMSO (*5, 6*). Hydrolysis of GTP molecule to GDP facilitates the process of polymer formation (*7*). However, exactly how the whole process of polymerization is promoted and controlled is not well understood.

A peculiarity of the tubulin primary structure is the surfeit of charged residues in the carboxy terminal segments. Almost 40% of all glutamates and 20% of all aspartates in tubulin are present in this region. The charges largely play an inhibitory role in the polymerization to microtubule. In fact, their chemical modification causes an enhanced ability to polymerize (*8*). The removal of these tails greatly increases the propensity of tubulin polymerization, although not

necessarily to polymers of right morphology (*9−11*). The flexible tail probably interacts with some region of the main globular region of the protein in a magnesium dependent manner (*1*), causing inhibition (*12*) of protein−protein association necessary for polymerization.

In addition to having a significant impact on the polymerization process, the tails also profoundly influence other properties, for example, colchicine binding (*13, 14*), bis-ANS binding (*15, 16*), and protein aging (*17*). Influence of the tail region on colchicine−tubulin interaction has been studied in some detail. Removal of the tail region lowers the activation energy of the colchicine binding. Interestingly, a similar effect on colchicine−tubulin interaction is seen when the pH is lowered, suggesting that perhaps the tail−body association is pH dependent (S. Chakrabarti and B. Bhattacharyya et al., manuscript in preparation). It is possible and perhaps likely that this and many other effects originate from the putative tail−body interaction, suggesting that an understanding of these phenomena from a structural point of view may advance our understanding of tubulin function significantly. In this paper, we have investigated a pH dependence of the conformation of a α-tubulin tail peptide, its broader implications for tail−body interaction and its effect on colchicine−tubulin interaction.

---

* To whom all correspondence should be addressed. FAX: +91-33-3344886.
§ Department of Biochemistry.
‡ Department of Biophysics.

MATERIALS AND METHODS

Materials. The 13-mer peptide CVEGEGEEEGEEY corresponding to the last 12 residues of α-tubulin and containing a N-terminal cysteine was a gift from Dr. E. Appella and Dr. K. Sakaguchi (National Institutes of Health, Bethesda, Maryland) and was synthesized using solid-phase methodology. The homogeneity of the peptide was characterized by reverse-phase HPLC and amino acid analysis.

NMR Experiments. The peptide was dissolved in 50 mM potassium phosphate buffer, pH 7, containing 10% D_2O and all NMR experiments were carried out under this solution conditions at 5 °C, unless stated otherwise. For pH-dependent measurements, the peptide was dissolved in 50 mM phosphate buffer of appropriate pH. All measurements were carried out in a Bruker DRX-500 NMR spectrometer. Water suppression was achieved by using WATERGATE pulse sequence. TOCSY spectra were performed using WATERGATE water suppression pulse followed by the spin-lock. NOESY spectra were also run using WATERGATE water suppression pulse (*18*). The diffusion measurement was carried out with stimulated echo based pulse sequence [90°-gradient pulse-90°-delay for diffusion-90°-gradient pulse-acquisition]. Typical delay for diffusion was set at 250 ms. The strength of the gradient pulse was varied and G^2 versus ln[intensity] was plotted. The temperature was set at 5 °C. Temperature coefficients were calculated from one-dimensional spectra taken at various temperatures and the obtained chemical shifts versus temperature data were fitted with linear regression.

Circular Dichroism. CD spectra were recorded on a JASCO J-600 spectropolarimeter in a 1-mm path length cuvette. A bandwidth of 2 nm and a time constant of 2 s were used in all measurements. All the CD spectra were measured in 50 mM phosphate buffer, pH 7.0 or 5.0, as described.

Refinement of Tubulin Model. The crystallographic model of tubulin (PDB code: 1TUB) determined by Nogales et al. (*19, 20*) is the basis for theoretical calculations in this paper. It is an unrefined model having only heavy atom positions derived using electron diffraction data at a resolution of 3.7 Å. Because of the low resolution, the modeling of the side chain is not very accurate; consequently, an objective interpretation of the results involving the atoms of the side chain is not always appropriate.

The starting model for our calculations was prepared by geometrically fixing the protons to the heavy atoms and optimizing their orientation by energy refinement with the CVFF force field (*21*) using the DISCOVER program (Biosym/MSI, 1995). The polypeptide-backbone coordinates of the refined model remained essentially the same as the original; however, there were some variations in the side-chain orientations of the residues at the surface.

Docking the Colchicine Molecule. The side-chains of amino acid residues are important for ligand−protein interaction. Since sufficiently reliable side-chain coordinates were not available, a two-step strategy was devised. This involved performing auto dock through grid search and thereafter manually refining the coordinates of the docked complex maintaining consistency with available biochemical data.

The automated docking using flexible ligand was performed using the program Dock (Version 4.0) (*22, 23*). Grid boxes of 0.3 Å on the side encompassing the tubulin dimer were constructed. The united atom model was employed to evaluate all van der Waals contacts using 6−12 potential functions. A distance-dependent dielectric constant (*24*) was used to calculate the atomic affinity and the final electrostatic potential energy map. The colchicine molecule was obtained from the small molecule crystal structure database at the Cambridge Crystallographic Data Centre (*25*). Initially, the colchicine and the tubulin models were put together on a graphics terminal. The colchicine molecule was arbitrarily placed at the proximity of Cys356 of the β-subunit, which is experimentally known to be a part of the binding site (*26*) (see also Figure 7 and related discussion later). The target binding region was thereafter demarcated by including all residues in the tubulin molecule that are within 20 Å of initial location. This way a gross region where the colchicine molecule can bind was delineated. Thereafter, an automated flexible docking was performed. Final colchicine binding site was based on energy score and sequence alignment information (see Results for details). An energy refinement was then carried out to reduce the number of bad contacts.

Structure Calculation. The peptide structure calculation was done using the program DYANA (*27*) on an Indigo workstation. Distance constraints for both the experiments at different pH values and 5 °C were derived using a 300 ms mixing time from NOESY spectra. Observed NOEs were translated into strong, weak, and medium categories, and these were converted into upper bound distances according to the type of protons involved. The lower bounds were limited to the sum of the van der Waals radii. Pseudoatom corrections were incorporated wherever necessary. The ϕ angles were translated from the J-coupling constants, and a range of $\phi \pm 10°$ was taken, except for the Gly residue. In cases where more than one ϕ value was derived, the one that is commonly found was used. These structures were further refined using their own backbone as templates. To accomplish this, the structures were subjected to minimization under conjugate gradient until the maximum derivative was less than 0.001 kcal/Å. A cluster analysis based on best-fit superposition of the polypeptide trace was performed to find out the groups of polypeptide sequences having similar conformation in the generated ensemble. A threshold value of 3.0 Å of the root-mean-square deviation of the equi-positioned atoms in the polypeptide chains was used to decide which pairs form a group.

Docking the α-Tubulin Tail. A docking grid was constructed whose extents covered a radius of 40 Å centered at the C^α atoms of the last residue (V440) visible in the X-ray determined structure. The idea was to demarcate the interaction site within an area that could be sterically accessible by the 13-mer peptide fragment if it were covalently bound to the residue V440. The grid boxes and the docking sites were calculated in a procedure similar to colchicine docking.

Potential interaction sites on tubulin can also be inferred by examining the electrostatic potential contours of the receptor surface. Consequently, the GRASP (*28, 29*) program was used to evaluate the electrostatic potential of the protein surface and visually evaluate if the docking sites provided electrostatic complementarity.
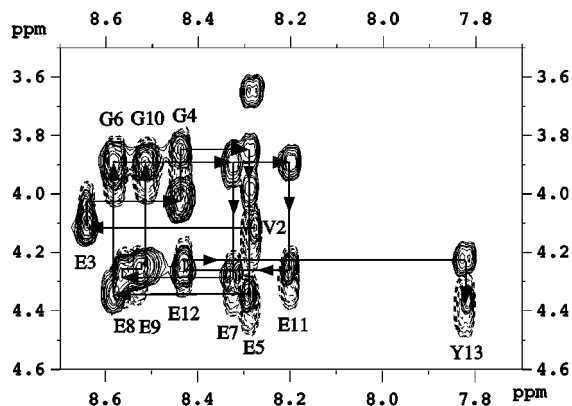
FIGURE 1: 500 MHz NOESY/TOCSY spectra overlay of the NH-αH region of tubulin α-tail peptide at 5 °C. The peptide was dissolved in 50 mM phosphate buffer, pH 5.0, at a concentration of 1.5 mM and the final pH was adjusted to 5. The mixing time for NOESY was 300 ms. Mixing time for TOCSY was 100 ms. Other experimental details are described in Materials and Methods. The broken lines are TOCSY, and the solid lines are NOESY.

RESULTS

It has been shown previously that tubulin−colchicine interaction is pH dependent, and pH dependency is lost when the α-tail is removed (*14*). Since the α-tail has been suggested to interact with the globular part of the body, a possible mechanism of pH dependence is through pH-dependent tail−body interaction. One way such interactions may be modulated is if the tail undergoes a pH-dependent conformational transition. Thus, we have investigated the dependence of the conformation of the α-tail peptide on pH. Figure 1 shows the NOESY/TOCSY plot of the α-tail peptide at pH 5. Under these conditions, all amide resonances can be completely assigned. A complete assignment was also obtained at pH 7 (data not shown). One of the important regions for conformational analysis is that of the NH−NH (i, i+1) NOEs. These distances are short in helices/turns and long (beyond NOE observable) in the extended state. Figure 2 shows the NH−NH regions of α-tail peptide at pH 5 and 7. At pH 5, several strong NH−NH NOEs can be observed, whereas no NH−NH NOEs are observed at pH 7. A straightforward interpretation is that at the lower pH, the peptide has several residues having a Ramachandran angle in the helical range.

Chemical shift changes and temperature coefficients of amide protons can provide important information about conformational change and its nature. Chemical shifts of α-H atoms in a peptide are important monitors of secondary structures. Figure 3A shows the change of chemical shift of the 13-residue peptide that occurs upon shift of pH 7 to pH 5. Several residues, 3, 5, 11 and 12, show a significant change of chemical shift upon a shift to pH 5. Some of these changes may be due to protonation of glutamic acid side-chain carboxyl group and some could be due to change of conformation. Since some α protons show an upfield shift, whereas some show a downfield shift, it is likely that part of the shift originates from conformational changes. Temperature coefficients provide indications about the relative exposure of amide protons. Figure 3B shows the temperature coefficients of several amide protons (the ones that can be resolved in one-dimensional spectra). It is generally accepted that for amide protons that are protected from solvent, the
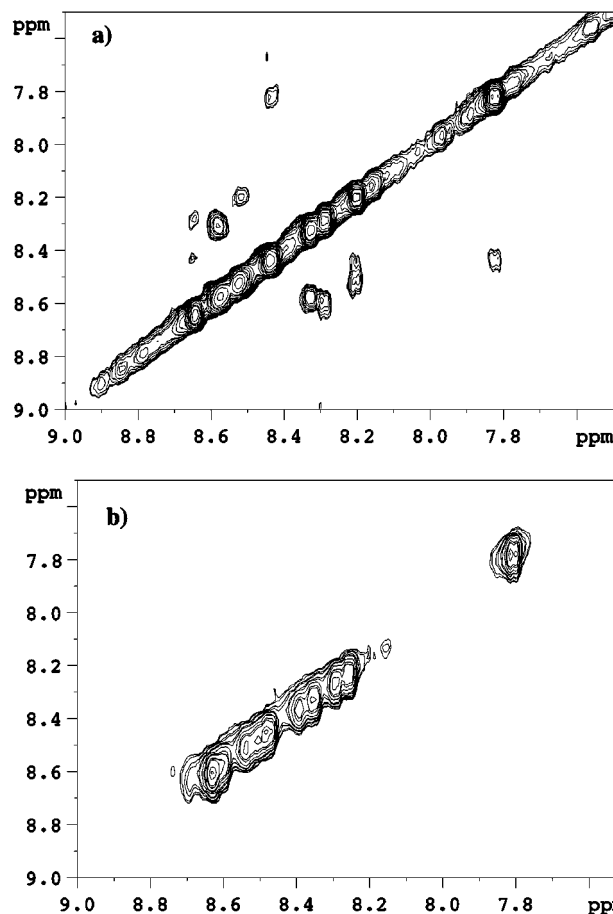

FIGURE 2: 500 MHz NOESY spectra of the NH−NH region of tubulin α-tail peptide at 5 °C at (a) pH 5.0 and (b) pH 7. Experimental details are as described in caption of Figure 1.

temperature coefficient falls below 5 ppb/°K. Several of the amide protons at pH 5 have temperature coefficients below 5 ppb/°K or near this value, suggesting that several protons have some degree of protection from the solvent. Only one amide proton at pH 7 shows temperature coefficients below 5 ppb/°K (data not shown). This supports the idea that at pH 5, the peptide has a compact structure.

Translational diffusion constants can provide important information about the hydrodynamic radius of molecules and thus indicate the degree of compactness in proteins and peptides (*30*). Figure 4 shows the ln[intensity] versus G^2 plot for valine methyl resonance of the peptide at pH 7 and pH 5. The best-fit lines are clearly different. The translational diffusion constant values ($D_{20,W}$) calculated from the slopes are 20.35×10^{-7} cm^2 s^{-1} and 15.46×10^{-7} cm^2 s^{-1}, for pH 5 and 7, respectively. Higher diffusion coefficient at pH 5 when compared to pH 7 indicates a more compact structure at pH 5. To have a better idea about the shape of the peptide at pH 5, we calculated the Perrin factor from the translational diffusion coefficient values. The Perrin factor is 1.25 at pH 5 corresponding to an axial ratio of 1:6 for a prolate elipsoid. In contrast, the Perrin factor is 1.65 at pH 7 corresponding to an axial ratio of greater than 1:15 (*30*). This indicates that upon a shift to pH 5, the peptide undergoes a conformational transition that is significantly more compact that the extended structure, prevalent at pH 7.

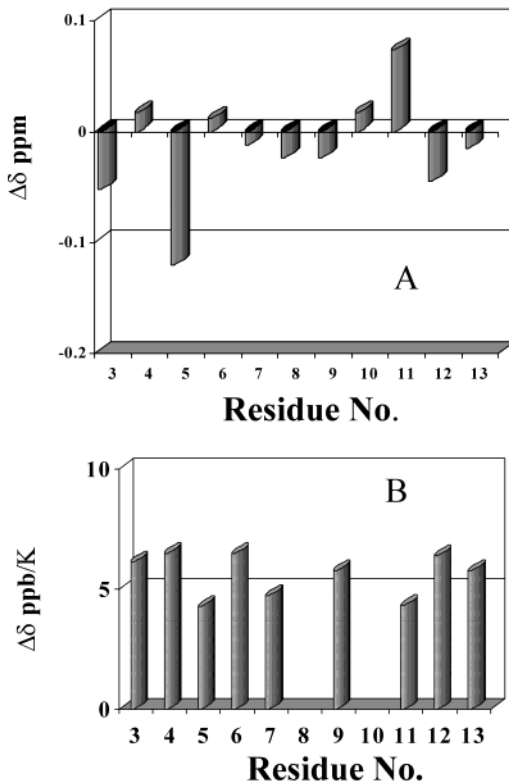Another way of looking at disorder−order transitions is to look at the far-UV CD spectrum. Figure 5 shows the

FIGURE 3: (A) Chemical shift difference of α-protons of the 13-residue peptide at pH 7 and 5 and (B) temperature coefficients of several amide protons of the same peptide at pH 5. Chemical shift differences are derived from TOCSY spectra at two pHs and taken at 5 °C. The temperature coefficients are derived from one-dimensional spectra taken at several temperatures at two different pHs. The solution conditions are as described in the caption of Figure 1.
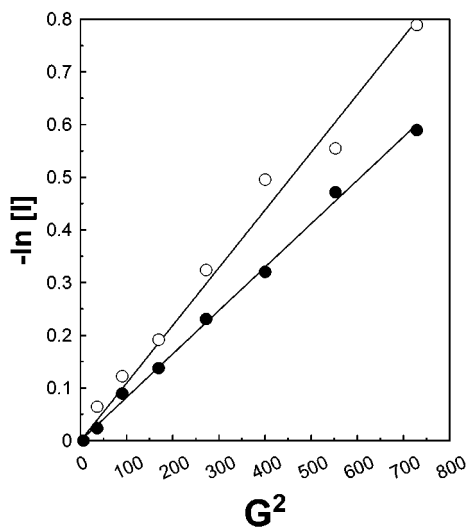

FIGURE 4: ln[intensity] versus G^2 plot for measurement of translational diffusion constant of the peptide at pH 5 (- -○- -) and pH 7 (- -●- -). The diffusion measurement was carried out with stimulated echo based pulse sequence [90°-gradient pulse-90°-delay for diffusion-90°-gradient pulse-acquisition] at 5 °C. The solution conditions are as given in the caption of Figure 1.

circular dichroism spectra of the α-tail peptide at pH 5 and 7. A significant decrease of CD signal in the range of 210−220 nm is seen. Because of the presence of the C-terminal tyrosine, the far UV circular dichroism spectrum of the α-tail peptide may a have large contribution from the single C-terminal tyrosine (*31*) and makes quantitative analysis very
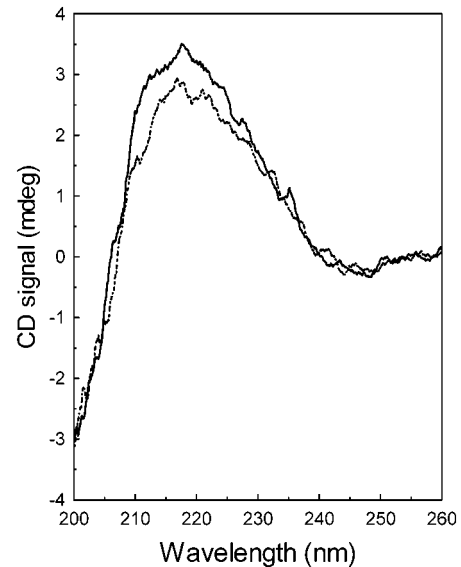

FIGURE 5: Circular dichroism spectra of the α-tail peptide at two different pHs, 7.0 (solid line) and 5.0 (broken line). The spectra were taken at ambient temperature. The peptide concentrations were 50 μM. Solution conditions were 50 mM potassium phosphate buffer at ambient temperature which was 25 ± 1 °C.

difficult. However, the difference of the two spectra is negative in the 210−220 region, not inconsistent with an increase of order.

The distance and angle constraint obtained from NOESY and coupling constants (obtained directly from one-dimensional spectra) are used in DYANA to obtain structures consistent with NMR-derived constraints. Figure 6 shows a cluster from an ensemble of structures obtained from data obtained at pH 5. It is clear that at pH 5, the structures show significant convergence. The structures at pH 5 are much more compact than either the fully stretched peptide or the representative structures obtained at pH 7 (data not shown).

Jiminez et al. (*32*) carried out investigations on the solution conformation of the functionally relevant C-terminal regions of α- and β-tubulin, corresponding to the amino acid polypeptide sequences 404−451 (end) and 394−445 (end) of the main vertebrate isotypes of α- and β-tubulin, respectively. They noted that the conformation of the fragments were largely helical in the middle with unstructured ends. The peptide sequence studied here was found to be in extended form at pH 7 (*32*) and is also consistent with crystallographic observations of disorder by Downing et al. (*33*).

Colchicine Docking Site. To elucidate how the tail may influence colchicine binding to tubulin, first the colchicine binding site on tubulin needs to be identified. Starting with random initial coordinates around Cys356β, the colchicine-binding site on tubulin was identified using automated docking methodology with high binding energy as the binding criterion. The binding site thus identified was close to His37β with several isoenergetic colchicine orientations. The colchicine binding reaction has an initial fast and reversible component, followed by tighter binding and quasi-irreversibility. The observed isoenergetic orientations within a confined area suggest that initial association could have broad substrate specificity. Indeed, many colchicine analogues are known to bind to the colchicine site without undergoing the second quasi-irreversible step.
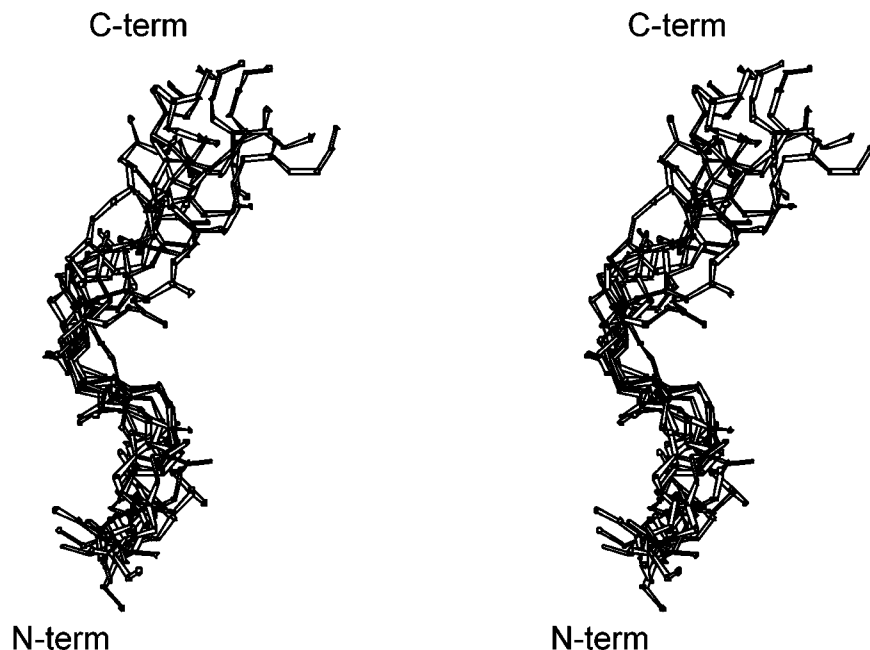
C-term

N-term

FIGURE 6: Several representative structures of α-tail peptide obtained from DYANA simulations and energy minimization in stereo representation. The DYANA simulation and energy minimization procedures are described in Materials and Methods.
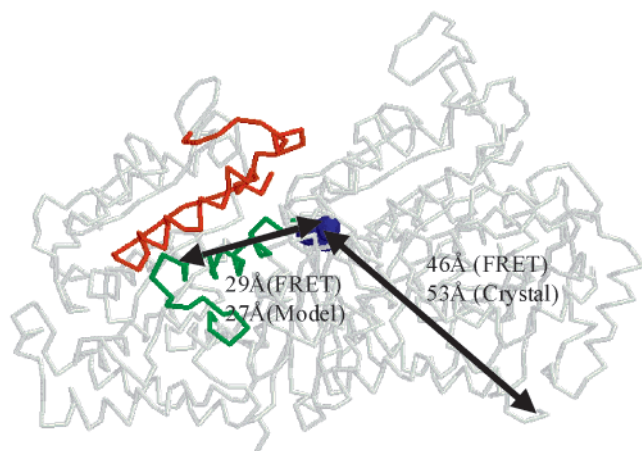

FIGURE 7: Location of the colchicine binding site on the tubulin crystal structure. The blue colored region is the colchicine binding site, whereas the green and brown colored segments are the peptides that are cross-linked with colchicine. The distance indicated by the arrow on the right-hand side is from colchicine to ruthenium red, while the other is between colchicine and paclitaxel.

Many experimental observations are supportive of this location of the colchicine binding site. Polypeptide sequences from 1 to 46 and 213−242 of the β-subunit are photo-crosslinked to colchicine, suggesting they are proximal to the colchicine binding site (*34*). These two peptide fragments are also found close to the colchicine docking site. Distances obtained from fluorescence energy transfer experiments between other ligands (depicted in Figure 7), which have been carried out by many investigators, agree with the colchicine binding site as shown in Figure 8 (*16*, *35*). To further refine the colchicine binding mode, we manually placed the colchicine molecule in a stacking position with His 37β and refined the coordinates. The choice of the residue His 37β was not arbitrary. A total of 56 β-tubulin sequences from diverse species were aligned using the ClustalW (1.4) program (*36*), and the dendrogram was drawn to identify their sequence similarity. In this, the histidine at

position 37 in the β-subunit is one of the residues that was most frequently found in colchicine-binding tubulin dimers and absent in nonbinding forms. Incidentally, another aromatic residue, Tyr, is just preceding the His residue and was found conserved in almost all the polypeptide sequences, as well. This suggests a strong correlation between the presence of histidine and the binding of the colchicine molecule. The docking site is a hydrophobic patch secured by a network of hydrogen bonds. The bulk of the molecule is associated with the β-subunit and the side-group attached to the B ring of colchicine hydrogen bonds with the α-subunit.

Tail−Body Interaction. The tail region of tubulin molecule is not visible in the crystal structure, suggesting that it occupies a broad range of conformational microstates. Previous studies have indicated that the tails interact with the main globular part of tubulin, but the nature of the interaction remains unclear (*1*, *37*). Because of high negative charge density in the tail peptides, it is likely that the interaction point in the main globular part is positively charged. Figure 9 shows that there are several sites having high electrostatic potential value, which could participate in charge−charge interaction leading to protein−protein association. Only one face of the protein is shown, as the other face does not have any significant positive charge clusters. All the charge clusters are approximately 30 Å away from Val440, the last residue seen in the crystal structure.

One way to assess the tail−body interaction is to run a Monte Carlo or a molecular dynamics simulation by co-valently fixing the body and the tail. An easier approach is to do a simple automated docking over a selected receptor surface. We used the second approach and the detached tail was docked in a radial span of 40 Å from the terminal residue (Val α-440) of the main body; within this distance the covalently bound tail could maximally migrate. The set of tail−body conformations generated by docking was divided into clusters, of which a major one involves the charge cluster centered around Lys394. The distance between Val440 and
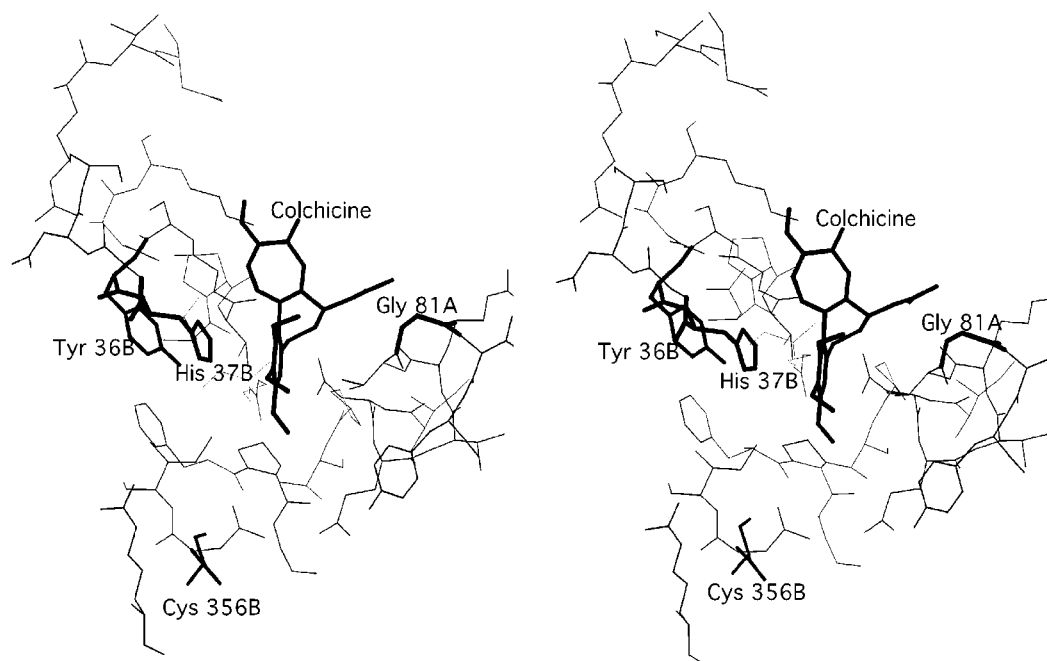
FIGURE 8: Putative colchicine binding site (showing protein residues within 8 Å of the docked molecule) on tubulin, shown in stereo. Histidine 37β makes a stacking contact primarily with the A-ring of colchicine. The A-ring is also proximal to Cys 356β. The acetamide group on ring B makes hydrogen-bonded contact with the main-chain atoms of Gly 81 located on a loop of α-subunit. Details of this and other possible hydrogen bonded interactions are as follows [protein atom followed by colchicine atom, N···O distance (Å) and NH···O angle (deg)]: Gly81α-NH···O6 (2.95, 140.9), Ser35β-NH···O2 (3.10, 155.7), and Arg79 α-O···N1 (3.42, 92.6).
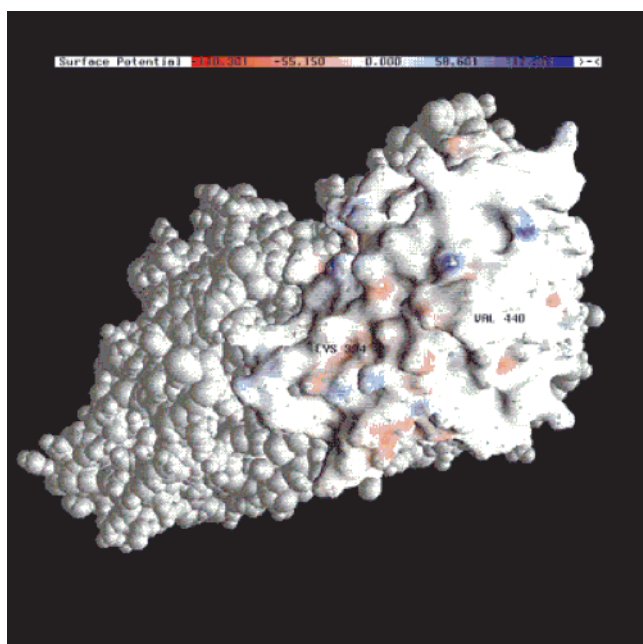

FIGURE 9: Electrostatic potential of tubulin surface (only the α-subunit is used) calculated using GRASP. The terminal residue visible in the X-ray structure (Val 440) and Lys 394, part of a positively charged cluster putatively interacting with the α-tubulin tail, are indicated.

Lys394 (for that matter, other positive charge clusters as well) can be spanned by an extended peptide of 12 residues long. Thus, the tail in high pH form can interact with Lys394 or any one of the other positive charge clusters shown. At the lower pH, the tail is more compact. The end-to-end distances of an ensemble of NMR structures falls between 10 and 30 Å (data not shown), suggesting it may be difficult for the lower pH structure to interact with the positive charge clusters

shown in Figure 9. It is interesting to note that Sternlicht and co-workers have previously proposed that the positive charge cluster containing Lys394 interacts with the negatively charged α-C-terminal tail (*38*).

DISCUSSION

The C-terminal tail region of α-tubulin has a profound effect on many aspects of tubulin function, although structural and mechanistic reasons for such effects are not well understood. One of the functions that the α-tail region influences is binding of colchicine. With the availability of crystal structure of tubulin, it is now possible to investigate how the α-tail exerts this effect. Although colchicine binding site on tubulin is not known from crystallographic data, docking calculations revealed that the colchicine binding site is at the α/β interface, diametrically opposite to the C-terminal tail region. Similar locations were also deduced from another study (*39*). The location is also in excellent agreement with a number of energy transfer and photolabeling experiments. Clearly, the C-terminal α-tail is too far from the colchicine binding site to have direct interactions with bound colchicine. It is very likely that interaction of the tail with other residues indirectly affect colchicine−tubulin interaction via a conformational change in the main body.

It has been known for a long time that β-tubulin tail sequences (isoforms) have a significant influence on many properties of tubulin, including colchicine binding. Recent data suggest such things may be true for α-tail (isoforms) as well. Clearly, this is a strong indication that both the α- and the β-tail−body interactions modulate many properties of tubulin (*40*, *41*) The existence of tail−body interactions has been demonstrated and suggested to be modulated by magnesium (*1*, *37*). However, exactly how the tail−body interactions modulate many aspects of tubulin function remains unsolved.
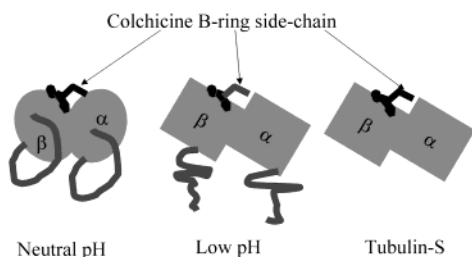
FIGURE 10: Model for tail−body interaction and its influence on tubulin−colchicine interaction. The subunit on the right is always α. At low pH, the β-subunit conformation was changed to a square one at low pH and in tubulin-S by analogy with the α. No information is available at present regarding conformation of the β-subunit under various conditions.

There is now increasing evidence that the A and C rings of colchicine bind to the β-subunit, while the exocyclic substituents of the B-ring bind to the α-subunit. Chaudhuri et al. (*42*) have made a similar suggestion and, in addition, have shown that the interaction of the B-ring leads to a change in conformation on the distal part of the α-subunit. From our docking experiments, it appears that A- and C-rings of the colchicine molecule interact with the β-subunit, whereas the exocyclic B-ring substituents interact with the amino acid residues of the α-subunit. The removal of exocyclic B-ring substituents (e.g., in desacetamido-colchicine) causes a lowering of the activation energy as well as the conversion of an entropy driven reaction to an enthalpy driven reaction (*43*). Thus, the increased activation energy and entropy driven character of colchicine−tubulin interaction noted above originate from interaction of exocyclic B-ring substituent with the amino acid residues on the α-subunit. This general structural pattern is also supported by the fact that thermodynamic and kinetic interaction patterns of colchicine with dissociated tubulin monomer is much like that of colchicine analogues without exocyclic B-ring substituents (*44*).

There is now increasing recognition that the α-tail has a significant influence on B-ring mediated conformational change in the α-subunit. It has been demonstrated previously that the removal of α-tail leads to major changes in colchicine binding parameters (*14*). For example, the colchicine off-rate constant increases approximately 5-fold at around neutral pH with a corresponding drop in the association constant. This clearly suggests that tail−body interaction alters colchicine binding. However, no significant changes are seen with colchicine analogues lacking B-ring side-chains upon removal of the α-tail, suggesting that such an effect originates from B-ring α-subunit interactions (S. Chakrabarti and B. Bhattacharyya, manuscript in preparation). At lower pHs, the off-rate constant is severalfold higher for colchicine, and very little effect is seen upon proteolytic removal of the tails (*14*). This is suggestive of nullification of tail−body interactions at lower pHs. Compaction of the tail at lower pHs offers an explanation of these effects. We propose that the compaction makes it sterically impossible for the tail to reach the site of interaction. Figure 10 sums up the above conclusions in the form of a model.

A number of reports suggest that a positive charge cluster in the globular part of tubulin is the interaction point with the negatively charged tail of α-tubulin. Modeling with the extended tail conformation (roughly equivalent to pH 7

conformation) suggests that a positive charge cluster around Lys394 can interact with the extended conformation of the negative charged tail. It is instructive that upon compaction of the tail at lower pH, the compact conformation cannot interact with this charge cluster. Thus, it is likely that nullification of this interaction leads to a conformational change in the globular part of tubulin and consequent loss of interaction with the exocyclic B-ring substituents. Many polycations promote polymerization along with the removal of the tail. It is possible that they bind to the tail and nullify the tail−body interaction. Since lowering of pH involves protonation of one or more aspartate/glutamate residues, binding of other polycations may also lead to charge shielding accompanied by a similar transition.

REFERENCES

1. Bhattacharya, A., Bhattacharyya, B., and Roy, S. (1994) *J. Biol. Chem. 269*, 28655−61.
2. Wolff, J., Sackett, D. L., and Knipling, L. (1996) *Protein Sci. 5*, 2020−8.
3. Kuznetsov, S. A., Gelfand, V. I., Rodionov, V. I., Rosenblat, V. A., and Gulyaeva, J. G. (1978) *FEBS Lett. 95*, 343−6.
4. Wolff, J. (1998) *Biochemistry 37*, 10722−9.
5. Hamel, E., and Lin, C. M. (1981) *Arch. Biochem. Biophys. 209*, 29−40.
6. Carlier, M. F., and Pantaloni, D. (1983) *Biochemistry 22*, 4814−22.
7. Vulevic, B., and Correia, J. J. (1997) *Biophys. J. 72*, 1357−75.
8. Mejillano, M. R., and Himes, R. H. (1991) *J. Biol. Chem. 266*, 657−64.
9. Bhattacharyya, B., Sackett, D. L., and Wolff, J. (1985) *J. Biol. Chem. 260*, 10208−16.
10. Maccioni, R. B. (1986) *Rev. Biol. Celular 8*, 1−124.
11. Serrano, L., Wandosell, F., de la Torre, J., and Avila, J. (1988) *Biochem. J. 252*, 683−91.
12. Serrano, L., Avila, J., and Maccioni, R. B. (1984) *J. Biol. Chem. 259*, 6607−11.
13. Avila, J., Serrano, L., and Maccioni, R. B. (1987) *Mol. Cell. Biochem. 73*, 29−36.
14. Mukhopadhyay, K., Parrack, P. K., and Bhattacharyya, B. (1990) *Biochemistry 29*, 6845−50.
15. Mazumdar, M., Parrack, P. K., Mukhopadhyay, K., and Bhattacharyya, B. (1992) *Biochemistry 31*, 6470−4.
16. Bhattacharya, A., Bhattacharyya, B., and Roy, S. (1996) *Protein Sci. 5*, 2029−36.
17. Sarkar, N., Mukhopadhyay, K., Parrack, P. K., and Bhattacharyya, B. (1995) *Biochemistry 34*, 13367−73.
18. Piotto, M., Saudek, V., and Sklenar, V. (1992) *J. Biomol. NMR 2*, 661−5.
19. Downing, K. H., and Nogales, E. (1998) *Curr. Opin. Cell Biol. 10*, 16−22.
20. Nogales, E., Whittaker, M., Milligan, R. A., and Downing, K. H. (1999) *Cell 96*, 79−88.
21. Dauber-Osguthorpe, P., Roberts, V. A., Osguthorpe, D. J., Wolff, J., Genest, M., and Hagler, A. T. (1988) *Proteins: Struct. Funct. Genet. 4*, 31−47.
22. Meng, E. C., Shoichet, B. K., and Kuntz, I. D. (1992) *J. Comput. Chem. 13*, 505−524.
23. Ewing, T. J. A., and Kuntz, I. D. (1997) *J. Comput. Chem. 18*, 1175−1189.

24. Mehler, E. L., and Solmajer, T. (1991) *Protein Eng. 4*, 903–910.
25. Allen, F. H., and Kennard, O. (1993) *Chem. Des. Autom. News 8*, 31–37.
26. Bai, R., Covell, D. G., Pei, X. F., Ewell, J. B., Nguyen, N. Y., Brossi, A., and Hamel, E. (2000) *J. Biol. Chem.* 2000.
27. Guntert, P., Mumenthaler, C., and Wuthrich, K. (1997) *J. Mol. Biol. 278*, 283–298.
28. Nicholls, A., Sharp, K. A., and Honig, B. (1991) *Proteins: Struct. Funct. Genet. 11*, 281–96.
29. Nicholls, A., and Honig, B. (1991) *J. Comput. Chem. 12*, 435–445.
30. Canor, C. C., and Schimmel, P. (1980) Biophysical Chemistry, W. H. Freeman, New York.
31. Chakrabartty, A., Kortemme, T., Padmanabhan, S., and Baldwin, R. L. (1993) *Biochemistry 32*, 5560–65.
32. Jimenez, M. A., Evangelio, J. A., Aranda, C., Lopez-Brauet, A., Andreu, D., Rico, M., Lagos, R., Andreu, J. M., and Monasterio, O. (1999) *Protein Sci. 8*, 788–99.
33. Downing, K. H., and Nogales, E. (1998) *Curr. Opin. Struct. Biol. 8*, 785–91.
34. Uppuluri, S., Knipling, L., Sackett, D. L., and Wolff, J. (1993) *Proc. Natl. Acad. Sci. U.S.A. 90*, 11598–602.
35. Ward, L. D., Seckler, R., and Timasheff, S. N. (1994) *Biochemistry 33*, 11900–8.
36. Thompson, J. D., Higgins, D. G., and Gibson, T. J. (1994) *Nucleic Acids Res. 22*, 3473–80.
37. Ortiz, M., Lagos, R., and Monasterio, O. (1993) *Arch. Biochem. Biophys. 303*, 159–64.
38. Szasz, J., Yaffe, M. B., Elzinga, M., Blank, G. S., and Sternlicht, H. (1986) *Biochemistry 25*, 4572–82.
39. Han, Y., Malak, H., Chaudhary, A. G., Chordia, M. D., Kingston, D. G., and Bane, S. (1998) *Biochemistry 37*, 6636–44.
40. Banerjee, A. (1999) *Biochemistry 38*, 5438–46.
41. Banerjee, A., Kasmala, L. T., Hamel, E., Sun, L., and Lee, K. H. (1999) *Biochem. Biophys. Res. Commun. 254*, 334–7.
42. Chaudhuri, A. R., Seetharamalu, P., Schwarz, P. M., Hausheer, F. H., and Luduena, R. F. (2000) *J. Mol. Biol. 303*, 679–692.
43. Chakrabarti, G., Sengupta, S., and Bhattacharyya, B. (1996) *J. Biol. Chem. 271*, 2897–901.
44. Banerjee, S., Chakrabarti, G., and Bhattacharyya, B. (1997) *Biochemistry 36*, 5600–6.